

# Rings and rigidity transitions in network glasses

Matthieu Micoulaut<sup>1</sup> and James C. Phillips<sup>2</sup>

<sup>1</sup>*Laboratoire de Physique Théorique des Liquides Université Pierre et Marie Curie,  
Boite 121 4, Place Jussieu, 75252 Paris Cedex 05, France*

<sup>2</sup>*Dept. of Physics and Astronomy, Rutgers University, Piscataway, N. J., 08854-8019*

(October 26, 2018)

Three elastic phases of covalent networks, (I) floppy, (II) isostatically rigid and (III) stressed-rigid have now been identified in glasses at specific degrees of cross-linking (or chemical composition) both in theory and experiments. Here we use size-increasing cluster combinatorics and constraint counting algorithms to study analytically possible consequences of self-organization. In the presence of small rings that can be locally I, II or III, we obtain two transitions instead of the previously reported single percolative transition at the mean coordination number  $\bar{r} = 2.4$ , one from a floppy to an isostatic rigid phase, and a second one from an isostatic to a stressed rigid phase. The width of the intermediate phase  $\Delta\bar{r}$  and the order of the phase transitions depend on the nature of medium range order (relative ring fractions). We compare the results to the Group IV chalcogenides, such as Ge-Se and Si-Se, for which evidence of an intermediate phase has been obtained, and for which estimates of ring fractions can be made from structures of high T crystalline phases.

Pacs: 61.20N-81.20P

## I. INTRODUCTION

A covalently bonded amorphous network progressively stiffens as its connectivity or mean coordination number  $\bar{r}$  increases<sup>1,2</sup>. The increase of connectivity can be achieved by adding cross-linking elements (such as As or Ge) to a starting chain network of S or Se. From a mechanical viewpoint, two-fold coordinated single bond chain networks are floppy because the number of nearest neighbor ( $r=2$ ) bonding constraints per atom is less than three, the degrees of freedom<sup>3</sup>. On the other hand, in the case of networks consisting only of tetrahedral units (such as amorphous four-fold coordinated silicon), the network is intrinsically rigid.

In single bond random networks, these simple observations have been described with success with a mean-field theory based on Maxwell constraint counting<sup>4</sup>. For  $r$ -fold coordinated atoms, the enumeration of atomic constraints  $n_c^\alpha = r/2$  and  $n_c^\beta = 2r - 3$ , respectively, due to bond stretching and bond-bending forces has shown that the number of zero-frequency (floppy) modes per atoms actually vanishes when the mean coordination number<sup>5,6</sup> of the network increases to the magic number of 2.4. At this point, the network sits at a mechanically critical point where the number of constraints per atom  $n_c = n_c^\alpha + n_c^\beta$  equals the number of degrees of freedom per atom. On the one hand, the exhaustion of all the degrees of freedom means that the network efficiently fills space. At the same time, because there are no excess constraints, the network can be thought of as globally isostatic.

Mean-field theory predicts onset of rigidity for  $\bar{r} > 2.4$ . Numerous experiments<sup>7,12,13</sup> have confirmed these simple predictions, especially in glass science where bulk chalcogenide glasses have been used as a benchmark to check these elegant ideas. Threshold behavior has been detected in structural<sup>8</sup>, vibrational<sup>9</sup>, thermal<sup>10</sup> and electronic<sup>11</sup> properties when  $\bar{r}$  approaches 2.4. Applications of rigidity theory have also been reported in various fields such as granular matter, biology and computational science<sup>14</sup>. However, recently it has been shown from Raman scattering and from phase-dependent measurements of the kinetics of the glass transition that two transitions<sup>15</sup> at  $\bar{r}_{c1}$  and  $\bar{r}_{c2}$  appear when the network stiffens. This suggests that the mean-field constraint counting alone (leading to the single

percolative transition) fails to describe completely network changes. These two transitions define an intermediate phase in which the connected structure continues to be stress-free<sup>16,17</sup> (isostatically rigid).

In this paper, we present a simple way to go beyond the mean-field description of rigidity and include local stress corrections. This is achieved by performing Maxwell constraint counting on size increasing structures, starting from the short-range level corresponding to the previous mean-field approach. One main advantage is that medium range order effects such as small rings can be taken into account in this construction. It appears from this analysis that these small rings mostly determine the nature of the intermediate phase and the values of the critical coordination numbers  $\bar{r}_{c1}$  and  $\bar{r}_{c2}$ , hence the width of the intermediate phase  $\Delta\bar{r} = \bar{r}_{c2} - \bar{r}_{c1}$ . To apply this construction, we choose the simplest case that can be built up, and which has received considerable attention in the context of rigidity, namely single-bonded Group IV chalcogenide glasses of the form  $B_xA_{1-x}$  with coordination numbers  $r_A = 2$  and  $r_B = 4$  defining the mean coordination number  $\bar{r} = 2 + 2x$ . We have used size-increasing cluster approximations (SICA) to construct these size-increasing structures and medium range order (MRO) on which we have realized constraint counting. As hoped, the analysis reveals two transitions: a first one, at which the number of floppy modes vanishes, is closely related to what has been previously obtained in the mean-field approach, and a second one (a “stress transition”), beyond which stress in the entire structure can no longer be avoided. The second transition can be obtained only under certain conditions which we detail below. We show that the orders of these phase transitions are different and depend on the fraction of ring structures. In between the two transitions, one can define an almost stress-free network structure for which the fraction of isostatic clusters can be computed.

The paper is organized as follows. In Section II, we show how to construct from small molecules size increasing clusters using SICA and perform Maxwell constraint counting on them. Section III is devoted to the results obtained from the construction, and the change in structure and energy with increasing connectivity. We discuss the results obtained and compare them with chalcogenide glasses in Section IV and finally, we extend the approach

to fast ionic conducting glasses in Section V.

## II. SIZE INCREASING CLUSTER APPROXIMATIONS

### A. Construction

In this section, we describe size increasing cluster approximations (SICA). This approach has been first introduced to describe the ring statistics and the intermediate range order in amorphous semi-conductors<sup>18</sup> such as  $B_2O_3$  but other applications have been considered such as the high temperature formation of fullerenes<sup>19</sup> and the cell distribution in quasi-crystals<sup>20</sup>. In principle, any structural quantity that is computed when one increases the size of a given structure (or a starting network) converges to its “true” value if the size becomes almost infinite. In practice, one hopes that the convergence is rapid enough to give reasonable values for medium-sized clusters, yielding information about MRO structures. In quasi-two-dimensional  $v - B_2O_3$  clusters having ten boron atoms allows one to obtain a fraction of boron atoms trapped in boroxol rings which is in very fair agreement with experiment<sup>18</sup>, but larger clusters may be needed for three-dimensional networks.

The basic level of the SICA construction is the restricted mean-field approximation where the probability of the short range order structure is derived from the macroscopic concentration, assuming that the cations and anions alternate in the network (chemical ordering). This basic level is denoted by  $l = 1$ . Then, we construct  $l = 2$ ,  $l = 3$  etc. and compute the corresponding probabilities in the Canonical Ensemble with particular energy levels  $E_i$  corresponding to bond creation between the ( $l = 1$ ) short range order molecules which are used as building blocks from step ( $l = 1$ ) (corresponding in  $Ge_xSe_{1-x}$  also to the reported mean-field approach<sup>3</sup>) to arbitrary  $l$ . The construction is supposed to be realized at the formation of the network, when  $T$  equals the fictive temperature  $T_f$  so that Boltzmann factors of the form  $e_i = \exp[-E_i/T_f]$  will be involved in the probabilities<sup>21</sup>. Since we expect to relate the width of the intermediate phase to the ring fraction, we will restrict

our present study to Group IV chalcogenides of the form  $Si_xSe_{1-x}$ . For the latter, there is strong evidence that at the stoichiometric concentration  $x=0.33$  a substantial amount of edge-sharing  $SiSe_{4/2}$  tetrahedra<sup>22,23</sup> can be found.

In order to study Group IV chalcogenides, we select basic units such as the  $A_2$  (i.e.  $Se_2$ ) chain fragment and the stoichiometric  $BA_{4/2}$  molecule (e.g.  $GeSe_{4/2}$  which is the majority local structure at  $x = 0.333$ ). These basic units have respective probabilities  $1 - p$  and  $p = 2x/(1 - x)$ ,  $x$  being the macroscopic concentration of the Group IV atoms. The energy levels are defined as follows. We associate the creation of a chain-like  $A_2 - A_2$  structure with an energy gain of  $E_1$ ,  $A_2 - BA_2$  bondings with an energy gain of  $E_2$  and corner-sharing (CS) and edge-sharing (ES)  $BA_{4/2}$  tetrahedra or any ring structure respectively with  $E_3$  and  $E_4$ . The energy  $E_4$  will be used to change the fraction of edge-sharing relative to corner-sharing tetrahedra. The probabilities of the different clusters have statistical weights  $g(E_i)$  which can be regarded as the degeneracy of the corresponding energy gain and correspond to the number of equivalent ways a cluster can be constructed. For the step  $l = 2$ , four different clusters can be obtained (see fig. 1) and their probabilities are given as follows:

$$p_1 = \frac{4(1-p)^2 e_1}{4(1-p)^2 e_1 + 16p(1-p)e_2 + p^2(16e_3 + 72e_4)} \quad (2.1)$$

$$p_2 = \frac{16p(1-p)e_2}{4(1-p)^2 e_1 + 16p(1-p)e_2 + p^2(16e_3 + 72e_4)} \quad (2.2)$$

$$p_3 = \frac{16p^2 e_3}{4(1-p)^2 e_1 + 16p(1-p)e_2 + p^2(16e_3 + 72e_4)} \quad (2.3)$$

$$p_4 = \frac{72p^2 e_4}{4(1-p)^2 e_1 + 16p(1-p)e_2 + p^2(16e_3 + 72e_4)} \quad (2.4)$$

out of which the concentration of B atoms  $x^{(2)}$  can be computed:

$$x^{(2)} = \frac{p_2 + 2(p_3 + p_4)}{4 - p_2 - 2(p_3 - p_4)} \quad (2.5)$$

Due to the initial choice of the basic units, the energy  $E_2$  will mostly determine the probability of isostatic clusters since the related Boltzmann factor  $e_2$  is involved in the probability

(2.2) of creating the isostatic  $BA_4$  cluster (a  $A_2 - BA_{4/2}$  bonding). This means that if we choose to have  $E_2 \ll E_1, E_3, E_4$ , the network will be mainly isostatic in the range of interest.

For the next steps, care has to be taken in order to count the possible isomers produced from different pathways (e.g. in fig. 1, the six-membered ring with two B atoms can be produced out of  $p_2$  and  $p_3$ ). More generally, increasing steps will lead to clusters with stoichiometry  $Ge_nSe_{2l}$  and probability proportional to  $p^n(1-p)^{l-n}$  with  $n = 0..l$ . The corresponding statistical weights depend much more on the way the clusters are created and have therefore no general formula depending on  $n$  or  $l$ . However, for the pure edge-sharing tetrahedra chain, it can be easily checked that its probability is proportional to  $72 \times 24^{l-2} p^l e_4^{l-1}$ . Another simple example is provided by the  $Se$  chain whose probability is  $4^{l-1}(1-p)^l e_1^{l-1}$ .

It is obvious that all the cluster probabilities will depend only on two parameters (i.e. the factors  $e_1/e_2$  and  $e_3/e_2$ ) and eventually  $e_4/e_2$  if one considers the possibility of edge-sharing (ES) tetrahedra or rings. One of the two factors can be made composition dependent since a conservation law for the concentration of  $B$  atoms  $x^{(l)}$  can be written at any step  $l$  of the SICA construction<sup>24</sup>:

$$x^{(l)} = x \tag{2.6}$$

This means that either the fictive temperature  $T_f$  or the energies  $E_i$  depends<sup>21</sup> on  $x$  but here only the  $e_i(x)$  (or  $e_i(\bar{r})$ ) dependence is relevant for our purpose.

The construction has been realized up to the step  $l = 4$  which already creates clusters of MRO size.

## B. Maxwell cluster constraint counting

On each cluster one can count Maxwell constraints by enumeration of bond-bending and bond-stretching constraints and calculation of the corresponding expressions of  $n_c^\alpha$  and  $n_c^\beta$ . Of particular importance are the structures containing a ring (see Fig. 1), because special

care has to be taken to avoid the counting of redundant constraints<sup>5</sup>. To illustrate this, let us consider an isolated triangle (i.e. a three-membered ring) having a 2-fold atom at each of its vertices. Of course, this triangle can be completely defined by three independent variables (e.g. two lengths and one angle). Performing constraint counting on the atoms will give three bond-stretching and three bond-bending constraints, yielding three redundant constraints. This means that for a three-membered ring, one has to remove three constraints from the global counting. For the four-membered ring, this correction is of two constraints, and for a five-membered ring, of one.

For each step  $l$ , we have computed the total number of constraints  $n_c^l$ :

$$n_c^{(l)} = \frac{\sum_{i=1}^{\mathcal{N}_l} n_{c(i)} p_i}{\sum_{i=1}^{\mathcal{N}_l} N_i p_i} \quad (2.7)$$

where  $n_{c(i)}$  and  $N_i$  are respectively the number of constraints and the number of atoms of the cluster of size  $l$  with probability  $p_i$ .  $\mathcal{N}_l$  is the total number of clusters of size  $l$ . At step  $l = 2$ , it is easy to check that:

$$n_c^{(2)} = \frac{4p_1 + 15p_2 + 22p_3 + 20p_4}{2p_1 + 5p_2 + 6(p_3 + p_4)} \quad (2.8)$$

We have determined either  $e_1/e_2$  or  $e_3/e_2$  by solving equ. (2.6), and once these factors become composition dependent, it is possible to compute the probabilities  $p_i$  as a function of composition and find for which concentration  $x$  (or which mean coordination number  $\bar{r}$ ) the system reaches optimal glass formation where the number of floppy modes  $f_l = 3 - n_c^{(l)}$  vanishes.

### III. RESULTS

#### A. Structural properties

In this section, we consider the solutions of the SICA construction under various structural possibilities.

The simplest case is random bonding, which is obtained when the cluster probabilities  $p_i$  are only given by their statistical weights  $g(E_i)$ . This would for example reduce the probability  $p_4$  in equ. (2.4) to

$$p_4 = \frac{18p^2}{(1+p)^2 + 18p^2} \quad (3.1)$$

with  $p = 2(\bar{r} - 2)/(4 - \bar{r})$ . A single solution is obtained for the glass optimum point defined by the vanishing of the number of floppy modes  $f = 0$  at all SICA steps, in the mean coordination number range [2.231,2.275], slightly lower than the usual mean-field value of 2.4. Since there is only one solution, there is no intermediate phase in the case of random bonding.

Self-organization of the network can be obtained by starting from a floppy cluster of size  $l$  (e.g. a chain-like structure made of a majority of A atoms), and allowing the agglomeration of a new basic unit onto this cluster to generate the cluster of size  $l+1$  only if the creation of a stressed rigid region can be avoided on this new cluster. This happens when two  $BA_{4/2}$  basic units are joined together on a given cluster. With this rather simple rule, upon increasing  $\bar{r}$  one accumulates isostatic rigid regions on the size increasing clusters because  $BA_{4/2}$  units are only accepted in  $A_2 - BA_{4/2}$  isostatic bondings with energy  $E_2$ . On the opposite side, one can start at high concentration, close to the mean coordination number of  $\bar{r} = 2.67$  and follow the same procedure but in opposite way, i.e. with adding A atoms, one allows only bondings which lead to isostatic rigid or stressed rigid regions, excluding systematically the possibility of floppy  $A_2 - A_2$  bondings.

In the case of self-organized clusters, the simplest case to be studied is the case of dendritic clusters, where no rings are allowed (achieved by setting  $e_4$  to zero). For an infinite size  $l$ , this would recover the results from Bethe lattice solutions or Random Bond Models<sup>25</sup> for which rings are also excluded in the thermodynamic limit<sup>26</sup>. A single transition for even  $l$  steps at exactly the mean-field value  $\bar{r} = 2.4$  is obtained whereas for the step  $l = 3$ , there is a sharp intermediate phase defined by  $f = 0$  (still at  $\bar{r} = 2.4$ ) and the vanishing of floppy regions (i.e.  $e_1/e_2$  is zero) at  $\bar{r} = 2.382(6)$ . Once the probabilities of floppy, isostatic rigid



and stressed rigid clusters as a function of the mean coordination number are computed, it appears that the network is entirely isostatic at the point where  $f = 0$  (solid line, fig. 2). There the number of degrees of freedom per atom is exactly three.

The intermediate phase shows up if a certain amount of medium range order (MRO) is allowed. This is realized in the SICA construction by setting the quantity  $e_4/e_2$  non zero, i.e. edge-sharing (ES) tetrahedra  $BA_{4/2}$  leading to four-membered rings  $B_2A_4$  can now be created at the growing cluster steps. This means also that if stress should be created when  $\bar{r}$  is increasing, then it should be only in ring structures and not by two corner-sharing connected  $BA_{4/2}$  tetrahedra.

Two transitions are now obtained for every SICA step. The first one lies always around the mean coordination number  $\bar{r}_{c1} = 2.4$  where the number of floppy modes  $f$  vanishes. The second transition is located at  $\bar{r}_{c2}$  and is a new feature of rigidity theory. When starting from a floppy network and progressively stiffening the network and requiring self-organization, the network will reach a point beyond which stressed rigid bondings outside of ring structures can not be avoided anymore. This point is a stress transition. We show in fig. 2 the  $l = 2$  result where  $f = 0$  at  $\bar{r}_{c1} = 2.4$  for different fractions of ES tetrahedra, defining an intermediate phase  $\Delta\bar{r}$ . We should also stress that even for a non-zero ES fraction,  $f = 0$  is always obtained at  $\bar{r} = 2.4$  for  $l = 2$ . From this analysis, it appears that the first transition at  $\bar{r}_{c1}$  does not depend on the ES fraction, as well as the fraction of stressed rigid clusters in the structure. In fig. 2, the probabilities of the related stressed rigid clusters for a non-zero ES fraction can of course be obtained from the floppy and isostatic ones since the sum of all probabilities is equal to one.

To ensure continuous deformation of the network when B atoms are added while keeping the sum of the probability of floppy, isostatic rigid and stressed rigid clusters equal to one, the probability of isostatic rigid clusters connects the isostatic solid line at  $\bar{r}_{c2}$ . Stressed rigid rings first appear in the region  $\bar{r}_{c1} < \bar{r} < \bar{r}_{c2}$  while chain-like stressed clusters (whose probability is proportional to  $e_3$ ) occur only beyond the stress transition, when  $e_3 \neq 0$ . This means that within this approach, when  $\bar{r}$  is increased, stressed rigidity nucleates through the

network starting from rings, as ES tetrahedra or small rings. It is easy to see from fig. 2 that the width  $\Delta\bar{r} = \bar{r}_{c2} - \bar{r}_{c1}$  of the intermediate phase increases with the fraction of ES. This can be extended to any MRO fraction (fig. 3) and it shows that  $\Delta\bar{r}$  is almost an increasing function of the ES fraction as seen from the result at SICA step  $l = 4$ . Since there is only a small difference between allowing only four-membered rings (ES) (lower dotted line) or rings of all sizes (upper dotted line) in the clusters, we conclude that the ES mostly determine the stress transition and hence the width.

Finally, one can see from fig. 2 and the insert of fig. 3 that the probability of isostatic clusters is maximum in the window  $\Delta\bar{r}$ , and almost equal to 1 for the even SICA steps, providing evidence that the molecular structure of the network in the window is almost stress-free. The point at which  $f = 0$  shifts slightly around  $\bar{r} = 2.4$  with the SICA step  $l$  (e.g. see the insert of fig. 3).

## B. Constraint free energy

From the cluster distribution obtained by the SICA, it is also possible to compute the constraint-related free energy, following the approach reported by Naumis<sup>27</sup>. Here, we have kept from the internal energy of the network only the part related to energy of the elastic deformations of the network, removing the contributions from the harmonic vibrations of the atoms and the anharmonic contributions which are irrelevant for our purpose (however, see<sup>27</sup>). This idea is also consistent with the work of Duxbury and co-workers who showed that the number of floppy modes behaves as a free energy for both rigidity and connectivity percolation<sup>28</sup>. The entropy of the network can be evaluated as a Bragg-Williams term from the distribution of cluster probabilities  $p_i$  at step  $l$ .

$$F_l = U_l - TS_l = Nk_B T f_l + Nk_B T \sum_{i=1}^{N_i} p_i \ln p_i \quad (3.2)$$

where  $f_l = 3 - n_c^{(l)}$  is the number of floppy modes computed following equ. (2.7). Since we have expressed the latter quantity as a function of the mean coordination number  $\bar{r}$  and

since the probabilities can also be expressed as a function of  $\bar{r}$ , the free energy can be plotted as a function of  $\bar{r}$  in the case of self-organization. Figure 4 shows the constraint related free energy  $F_l$  for two non-zero ES fractions.

It appears from the figure that the second transition at  $\bar{r}_{c2}$  (the “stress transition”) is a first order transition while the first transition at  $\bar{r}_{c1}$  is weakly second order. Moreover, as one can see from the insert, the first transition at  $\bar{r}_{c1}$  progressively becomes first order in character when the rate of edge-sharing tetrahedra  $\eta$  is increased. On the other hand, the jump of  $F_l^{(1)}$  at  $\bar{r} = \bar{r}_{c2}$  is reduced when the ES fraction is increased (insert of fig. 4).

Both curves show a marked minimum of  $F_l$  in the range  $[\bar{r}_{c2}, 2.667]$  at a certain coordination number  $\bar{r}_e$  which signals an equilibrium state with respect to cross-linking. A major consequence of this result is that one may expect phase separation in the stressed rigid region leading for increasing cluster sizes to nano-scale phase separation in the network backbone. Close to  $\bar{r} = 2.667$ , the structure should therefore be made of B-poor clusters having the statistics of the local  $F_l$  minimum but also compensating B-rich clusters in order to still satisfy equ. (2.6). This structural change is driven by the entropic term appearing in equ. (3.2) since the energy of the elastic deformation of the network is zero in the stressed rigid phase. With increasing ES fraction, this equilibrium state shifts to the value 2.667. For a ES fraction of 1, equilibrium state and stoichiometric composition merge together. Experimental evidence of nanoscale phase separation is discussed in the following.

## IV. DISCUSSION

### A. The Boolchand Intermediate phase

As mentioned above, chalcogenide glasses are the first systems that have been carefully studied and the intermediate phase defined by the two transitions has been discovered by Boolchand in the context of self-organization<sup>15,16</sup>. SICA provides therefore a benchmark to check the results obtained. To be specific, Raman scattering<sup>15,29</sup> probes elastic thresholds

in binary  $Si_xSe_{1-x}$  or  $Ge_xSe_{1-x}$ . The germanium or silicon corner sharing mode chain frequencies change with mean coordination number  $\bar{r}$  of the glass network. These frequencies exhibit not only a change in slope at the mean coordination number  $\bar{r}_{c1} = 2.4$ , but also a first order jump at the second transition  $\bar{r}_{c2}$ . In germanium systems, the second transition is located around the mean coordination number of 2.52 whereas  $\bar{r}_{c2} = 2.54$  in Si based systems. For both systems, a power-law behavior in  $\bar{r} - \bar{r}_{c2}$  is detected (see fig. 5) for  $\bar{r} > \bar{r}_{c2}$  and the corresponding measured exponent is very close to the one obtained in numerical simulations of stressed rigid networks<sup>36</sup>. Moreover, these results clearly correlate with the vanishing between  $\bar{r}_{c1}$  and  $\bar{r}_{c2}$  of the non-reversing heat flow  $\Delta H_{nr}$  (the part of the heat flow which is thermal history sensitive) in MDSC measurements<sup>15,29</sup>.

The study of stoichiometric compounds such as  $SiSe_2$  or  $GeSe_2$  also leads to better understanding of medium range order. In the former, <sup>29</sup>Si NMR experiments have shown that most of the tetrahedra were part of long edge-sharing chains<sup>30</sup> in the glass.  $SiSe_2$  has different crystalline polymorphs which all exhibit a strong edge-sharing tendency<sup>31</sup>. The high temperature phase is made of 100% edge-sharing tetrahedral<sup>32</sup>, while different phases display a distribution in terms of NMR  $E^{(k)}$  functions (where the subscript  $k = 0, 1, 2$  refers to the number of tetrahedra shared by edges on a tetrahedron), but with a majority of  $E^{(2)}$  structures<sup>31,33</sup>. In the  $SiSe_2$  glass, the fraction of  $E^{(2)}$  has been found to be of the order<sup>34</sup> of 0.53. On the other hand, low temperature crystalline  $GeSe_2$  has no edge-sharing tetrahedral<sup>35</sup>, but glassy  $GeSe_2$  exhibits a companion Raman line associated with edge-sharing tetrahedra<sup>4</sup>).

The SICA approach has shown that the width  $\Delta\bar{r}$  of the intermediate phase increases mostly with the fraction of ES tetrahedra. We stress that the width should converge to a lower limit value of  $\Delta\bar{r}$  compared to the step  $l = 2$ , therefore one can observe the shift downwards when increasing  $l$  from 2 to 4. This limiting value is in principle attained for  $l \rightarrow \infty$ , or at least for much larger steps<sup>37</sup> than  $l = 4$ . For Si-Se,  $\Delta\bar{r} = 0.14$  is much more sharply defined than for Ge-Se ( $\Delta\bar{r} = 0.12$ ) consistent with the fact that the number of ES tetrahedra is higher in the former<sup>16</sup>.

## B. Nanoscale phase separation

Phase separation effects in glasses exhibit usually pronounced changes in physical properties and most studies have focused on thermally driven heterogeneities which can in some cases display bimodal glass transition temperatures. Here the separation effect results from a change in network connectivity which has its origin in the free energy minimum at  $\bar{r}_e$ .

It appears that these nano-scale phase separation have been revealed from compositional trends<sup>29</sup> of the glass transition temperature  $T_g$  because they display a maximum in  $T_g$  close to the stoichiometric concentration. Such a feature has been observed in Ge-Se<sup>15</sup>, As-Se<sup>38</sup> alloys, but not in Si-Se<sup>16</sup>. These  $T_g$  trends can be compared with spectroscopic (Raman<sup>39</sup>, Mössbauer<sup>29</sup>) data which also give evidence of broken chemical order, suggesting that the structure of stoichiometric glasses such as  $GeSe_2$  or  $As_2Se_3$  is made of a chalcogen rich majority phase and a compensating Ge- or As- rich phase. Furthermore, in the metal rich phase Ge-Ge or As-As bonds are present.

The difference between the Si-Se and the Ge-Se glass lies in the following. Since the Si-Se has a much higher ES fraction compared to Ge-Se, the value of its corresponding local constraint free energy equilibrium will lie very close to the value  $\bar{r} = 2.667$  (see insert of fig. 4). The Ge counterpart will have the same minimum at a lower value in the range  $[\bar{r}_{c2}, 2.667]$  because of fewer ES tetrahedra thus favouring the emergence of the chalcogen-rich phase when  $\bar{r}$  is increased. Our last comments brings us back to constraint counting. Since Si-Se is more weakly constrained than Ge-Se due to the higher amount of ES<sup>5</sup>, the glass transition temperature of the stoichiometric glass will be higher compared to Ge-Se.

## V. APPLICATION TO FAST IONIC CONDUCTORS

One interesting field of application of cluster construction and constraint counting algorithms is the field of fast ionic conductors (FIC)<sup>40,41</sup>, which has received considerable attention in the last fifteen years because of potential applications of these solid electrolytes

in all solid state electrochemical devices and/or miniaturized systems such as solid state batteries. An important step forward has been made by replacing the oxygen in usual oxide glasses by more polarizable chalcogenide atoms (S,Se mostly) which has increased the dc conductivity<sup>42</sup> in these systems by several orders of magnitude<sup>43</sup>, up to a value of about  $10^{-3} \Omega^{-1}.cm^{-1}$ . Surprisingly, the extension of constraint theory from network chalcogenide glasses such as  $As_xSe_{1-x}$  to ionic glasses has received little attention and to our knowledge, has been only reported for a few oxide glasses<sup>44,45</sup>. Elastic percolative effects in these types of networks have not been studied so far with the network change in solid electrolytes, although it is certainly fundamental for the understanding of the mobile carriers' motion since various models of conductivity<sup>46,47</sup> stress the importance of the mobility  $\mu$  in the contribution to conductivity. Obviously, the mobility is related to a local mechanical deformation of the network<sup>48</sup>, allowing a cation to move through holes in the structure. In terms of rigidity, one may therefore expect that the mobility  $\mu$  in a stressed rigid solid electrolyte should be substantially lower compared to the cation mobility in a floppy one, because in the latter floppy modes allow a local low energy deformation. The percolative effect of mobility should certainly show up in this kind of network so that the conductivity  $\sigma$  should display some particular behavior in the stress-free intermediate phase and at the two transitions.

The SICA approach can be applied to the present solid electrolyte case by considering the simplest binary conducting glass, which is of the form  $(1-x)SiX_2 - xM_2X$  with X an anion of Group VI (X=O,S,Se) and M an alkali cation (M=Li,Na,K,...). The free carriers are the  $M^\oplus$  cations. The local structure in these glasses can be determined by many different experiments and is usually described in terms of so-called  $Q^4$  and  $Q^3$  units, derived from NMR data<sup>49</sup>. The former corresponds to the usual silica tetrahedron made of one silicon and four Group VI atoms at the corner [e.g.  $SiSe_{4/2}$ ] while the latter has one additional anion bonded to the alkali cation [e.g.  $SiSe_{5/2}^\ominus Na^\oplus$ ] that does not connect anymore to the network (fig. 6). Although it is yet not clear what is the coordination number of the alkali cation<sup>50</sup>, it can be assumed that the strongest interaction of the alkali cation is the one related to the NBO. This means that the effective coordination number of  $M$  is taken as one, as suggested

by different authors<sup>45,51</sup>.

Starting from the local  $Q^4$  and  $Q^3$  units (with respective probabilities  $1 - p$  and  $p = 2x/(1 - x)$ ), the SICA probabilities can be evaluated for different steps of cluster sizes following the procedure described previously and taking into account the 1-fold M cations<sup>52</sup>. When constraint counting is performed, it appears that the creation of a  $Q^4 - Q^4$  connections leads to a stressed rigid cluster, while the  $Q^4 - Q^3$  and  $Q^3 - Q^3$  connections yield respectively isostatically stressed and floppy clusters. The SICA results show again that the intermediate phase exists only when a non-zero fraction of small rings is allowed in the self-organized structure. The corresponding results are displayed in fig. 7 for  $l = 2$  and work on higher SICA steps is in progress<sup>53</sup>. Rigidity nucleates here in a way opposite to network chalcogenides. The vanishing of the number of floppy modes defines the upper limit of the intermediate phase, while stressed rigidity outside of ring structures disappears for  $x > x_{c1}$ . This is consistent with the fact that the network is stressed rigid at low modifier concentration. However, the base network glass is stress free. In  $SiO_2$ , the Si-O-Si angle distribution is quite wide leading to broken bond-bending constraints on oxygen<sup>54</sup>, while in the  $SiS_2$  and  $SiSe_2$  glasses, the structure is mostly made out of edge-sharing  $SiSe_{4/2}$  or  $SiS_{4/2}$  tetrahedra<sup>30</sup> which are weakly stressed (i.e.  $n_c \leq 3.667$  a value which would be expected in a dendritic network at the mean coordination number  $\bar{r} = 2.667$  or concentration  $x = 0.333$ ) due to the 4-membered ring correction coming from the counting of redundant constraints<sup>5</sup>.

Increase of the alkali content leads to an increase of floppiness. In the oxide system  $(1 - x)SiO_2 - xM_2O$ , the width  $\Delta x$  should be very small or zero since the fraction of ES tetrahedra in the oxide systems is almost zero<sup>21</sup>. Still, percolative effects are expected at the concentration  $x = 0.2$  corresponding to the transition from rigid to floppy networks, a transition that has been observed in sodium tellurate glasses<sup>44</sup>. In sulfur and selenide glasses such as  $(1 - x)SiS_2 - xNa_2S$ , the width should be much broader because of the existence of the high amount of edge-sharing tetrahedra in the  $SiS_2$  or  $SiSe_2$  base networks<sup>34</sup>. For glasses with a high amount of ES tetrahedra, the lower limit at  $x_{c1}$  of the intermediate phase

is expected to decrease down to  $x = 0$  for the limiting case  $\eta = 1$ . In the sulfur base glass,  $^{29}\text{Si}$  NMR have shown that the fraction of ES tetrahedra should be about 0.5, slightly higher than in the selenide analogous system<sup>55,56</sup>.

From fig. 7, for  $\eta = 0.5$  one should observe a window of about  $\Delta x = 0.09$ . Unfortunately, conductivity, structural and thermal results<sup>57</sup> on these systems are only available for an alkali concentration  $x > 0.2$ . However, in the different silica based glasses, a rigidity transition has been observed<sup>58</sup> at the concentration  $x = 0.2$  which should provide guidance for forthcoming studies in this area.

Finally, temperature effects should be observable close to this transition. Since the concentration of alkali free carriers  $n_L$  depends on the temperature (the higher the temperature, the higher  $n_L$ ), an increase of the temperature  $T$  should lead to a decrease of the number of network constraints, the fraction of intact bond-stretching constraints  $n_c^\alpha$  of the alkali atom being proportional to  $1 - n_L$ . Consequently, a shift of the mechanical threshold ( $f = 0$ ) to the higher concentrations should result from an increase of  $T$ .

## VI. SUMMARY AND CONCLUSIONS

To summarize, we have shown in this article how stress change in molecular systems can be described using both cluster construction and constraint counting. This permits to go beyond the usual mean-field approach of rigidity and to obtain the two observed rigidity transitions. We have found that there is a single transition from floppy to rigid networks in a certain number of structural possibilities. An intermediate phase appears when a fraction of medium range order is allowed in self-organized networks and the order of the underlying phase transitions is first and second order, and depend also on the fraction of ES. Nano-scale phase separation appears in the stressed rigid phase and is driven by the cluster entropy. This separation leads to Group VI-rich clusters and chalcogen rich clusters when the stoichiometric composition is attained. Finally, extension of this approach to ionic conductors has been emphasized and should motivate new developments in this field.



- <sup>1</sup> W.J. Bresser, P. Suranyi and P. Boolchand, Phys. Rev. Lett. **56** (1986) 2493
- <sup>2</sup> P. Boolchand, Phys. Rev. Lett. **57** (1986) 3233
- <sup>3</sup> J.C. Phillips, J. Non-Cryst. Solids **34** (1979) 153
- <sup>4</sup> J.C. Phillips, J. Non-Cryst. Solids **43** (1981) 37
- <sup>5</sup> M.F. Thorpe, J. Non-Cryst. Solids **57** (1983) 355
- <sup>6</sup> H. He and M.F. Thorpe, Phys. Rev. Lett. **54** (1985) 2107
- <sup>7</sup> W.A. Kamitahara, R.L. Cappelletti, P. Boolchand, B. Halfpap, F. Compf, D.A. Neumann, H. Mutka, Phys. Rev. B **44** (1991) 94
- <sup>8</sup> S.S. Yun, H. Li, R.L. Cappelletti, P. Boolchand, R.N.ENZWEILER, Phys. Rev. **B39** (1989) 8702
- <sup>9</sup> K. Murase, T. Fukunaga, in *Defects in glasses*, Mater. Res. Soc. Symp. **61** (1986) 101
- <sup>10</sup> U. Senapati, A.K. Varshneya, J. Non-Cryst. Solids **185** (1995) 289
- <sup>11</sup> S. Asoka, E.S.R. Gopal, G. Parathasarathy, Phys. Rev. **B35** (1987) 8369
- <sup>12</sup> M. Tatsumisago, B.L. Halfpap, J.L. Green, S.M. Lindsay and C.A. Angell, Phys. Rev. Lett. **64** (1990) 1549
- <sup>13</sup> U. Senapati and A.K. Varshneya, J. Non-Cryst. Solids **185** (1995) 289; T. Wagner and S. Kasap, Phil. Mag. **B74** (1996) 667
- <sup>14</sup> see *Rigidity theory and applications*, M.F. Thorpe, P.M. Duxbury Eds. Fundamental Materials Research Series, Plenum Press/Kluwer Academic 1999
- <sup>15</sup> X. Feng, W.J. Bresser and P. Boolchand, Phys. Rev. Lett. **78** (1997) 4422

- <sup>16</sup> D. Selvenathan, W.J. Bresser, P. Boolchand, Phys. Rev. **B61** (2000) 15061
- <sup>17</sup> M.F. Thorpe, D.J. Jacobs, M.V. Chubynsky and J.C. Phillips, J. Non-Cryst. Solids **266-269** (2000) 859
- <sup>18</sup> M. Micoulaut, R. Kerner and D.M. dos Santos-Loff, J. Phys. Cond. Matt. **7** (1995) 8035
- <sup>19</sup> R. Kerner, K. Penson and K.H. Bennemann, Europhys. Lett. **19** (1992) 363
- <sup>20</sup> R. Kerner and D.M. dos Santos-Loff, Phys. Rev. **B37** (1988) 3881
- <sup>21</sup> F.L. Galeener, D.B. Kerwin, A.J. Miller and J.C. Mikkelsen Jr., Phys. Rev. **B47** (1993) 7760
- <sup>22</sup> M. Micoulaut, Physica **B212** (1995) 43
- <sup>23</sup> Z. Zhang and J.H. Kennedy, Solid St. Ionics **38** (1990) 217
- <sup>24</sup> P.J. Bray, S.A. Feller, G.E. Jellison and Y.H. Yun, J. Non-Cryst. Solids **38-39** (1980) 93
- <sup>25</sup> D.J. Jacobs and M.F. Thorpe, Phys. Rev. Lett. **80** (1998) 5451
- <sup>26</sup> M.F. Thorpe, D.J. Jacobs and M.V. Chubynsky in *Rigidity theory and applications*, edited by Plenum press/Kluwer Academic 1999
- <sup>27</sup> G.G. Naumis, Phys. Rev. **B61** (2000) 6105
- <sup>28</sup> P.M. Duxbury, D.J. Jacobs, M.F. Thorpe, C. Moukarzel, Phys. Rev. **E59** (1999) 2084
- <sup>29</sup> P. Boolchand and W.J. Bresser, Phil. Mag. **B80** (2000) 1757
- <sup>30</sup> L.F. Gladden and S.R. Elliott, Phys. Rev. Lett. **59** (1987) 908
- <sup>31</sup> A. Pradel, V. Michel-Lledos, M. Ribes and E. Eckert, Chem. Mater. **5** (1993) 377
- <sup>32</sup> E. Zintl, K. Loosen, Z. Phys. Chem. Leipzig **174** (1935) 301
- <sup>33</sup> M. Tenhover, M.A. Hazle, R.K. Grasseli, Phys. Rev. **B29** (1984) 6732
- <sup>34</sup> H. Eckert, J. Kennedy, A. Pradel and M. Ribes, J. Non-Cryst. Solids **113** (1989) 187

- <sup>35</sup> G. Dittmar, H. Schafer, Acta. Crysta. B**32** (1976) 2726
- <sup>36</sup> D.S. Franzblau and J. Tersoff, Phys. Rev. Lett. **68** (1992) 2172
- <sup>37</sup> M. Micoulaut, J. Molec. Liquids **71** (1997) 107
- <sup>38</sup> T. Wagner, S.O. Kasap, M. Vlcek, A. Sklenar, A. Stronski, J. Non-Cryst. Solids **227-230** (1998) 752
- <sup>39</sup> P. Boolchand, X. Feng, W.J. Bresser, J. Non-Cryst. Solids **233** (2001) 348
- <sup>40</sup> Z. Jinfeng and S. Mian-Zeng, *Materials for solid state batteries*, ed. B.V.R. Chowdari and S. Radhakrishna (1986) p. 487
- <sup>41</sup> S.W. Martin, Eur. J. Solid. St. Inorg. Chem. **28** (1991) 163
- <sup>42</sup> S.W. Martin, J.A. Sills, J. Non-Cryst. Solids **135** (1991) 171
- <sup>43</sup> S. Sahami, S. Shea and J. Kennedy, J. Electrochem. Soc. **132** (1985) 985
- <sup>44</sup> M. Zhang and P. Boolchand, Science **266** (1994) 1355
- <sup>45</sup> R. Kerner and J.C. Phillips, Solid State Comm. **117** (2000) 47
- <sup>46</sup> O. Anderson, D. Stuart, J. Am. Ceram. Soc. **37** (1954) 573
- <sup>47</sup> D. Ravaine, J.L. Souquet, Phys. Chem. Glasses **18** (1977) 27
- <sup>48</sup> L.F. Perondi, R.J. Elliott, R.A. Barrio and K. Kaski, Phys. Rev. **B50** (1994) 9868
- <sup>49</sup> J.F. Stebbins, J. Non-Cryst. Solids **106** (1988) 359
- <sup>50</sup> see for example *Structure, Dynamics and Properties of Silicate Melts*, Reviews in Mineralogy **32** (1995)
- <sup>51</sup> R. Narayanan, Phys. Rev. **B64** (2001) 134207
- <sup>52</sup> P. Boolchand, M.F. Thorpe, Phys. Rev. **B50** (1994) 10366

<sup>53</sup> F. Chaimbault, M. Micoulaut, Y. Vaills, unpublished

<sup>54</sup> J.F. Stebbins, P.W. MacMillan, *J. Non-Cryst. Solids* **160** (1993) 116

<sup>55</sup> A. Pradel, M. Ribes, *Solid St. Ionics* **18-19** (1986) 351

<sup>56</sup> A. Pradel, M. Ribes, *J. Non-Cryst. Solids* **131-133** (1991) 1063

<sup>57</sup> A. Pradel, J. Taillades, M. Ribes and H. Eckert, *J. Non-Cryst. Solids* **188** (1995) 75

<sup>58</sup> Y. Vaills, G. Hauret, Y. Luspin, *J. Non-Cryst. Solids* **286** (2001) 224

## List of Figures

- 1 From the short range order molecules ( $l = 1$ ) yielding the mean-field result to all clusters at  $l = 2$  and some MRO produced at  $l = 3$ . Isomers start to be created at step  $l = 3$ . Note the creation of medium range order such as edge-sharing tetrahedra or rings. Each boundary atom is counted half. . . . 23
- 2 Probability of floppy, isostatic stressed and stressed rigid clusters, as a function of the mean coordination number  $\bar{r}$  for different possibilities of medium range order. The solid line corresponds to the dendritic case while the broken lines correspond to a respective ES fraction at the stress transition of 0.156, 0.290 and 0.818. The filled square indicates the stress transition at the point  $\bar{r}_{c2}$  and the filled circle the point  $\bar{r}_{c1}$  that does not depend on the ES rate (see text for details). For clarity, we have removed the probabilities of stressed rigid clusters for non-zero ES fractions. . . . . 24
- 3 Width of the intermediate phase as a function of the fraction of medium range order at the stress transition for  $l = 2$  (solid line),  $l = 3$  (dashed line) and  $l = 4$  (dotted lines). The lower dotted line corresponds to a structure where only ES tetrahedra have been allowed. The insert shows the probability of isostatic clusters with mean coordination number for  $l = 3$  (dashed line) and  $l = 4$  (dotted line), compared to the shaded region defined by the  $\Delta\bar{r}$  from SICA analysis. The point defined by  $f = 0$  is shifted compared to  $l = 2$ . . . . 25
- 4 Upper panel: Free energy  $F_l$  of the system  $A_{1-x}B_x$  as a function of the mean coordination number  $\bar{r}$  for different fractions of edge-sharing units  $\eta$ . Open circles:  $\eta = 0.29$ , filled circles:  $\eta = 0.56$ . The insert shows the equilibrium coordination number  $\bar{r}_e$  with respect to the ES fraction (see text for details). Lower panel: the first derivative of the free energy  $F_l^{(1)}$  with respect to  $\bar{r}$  as a function of  $\bar{r}$ . . . . . 26

5	<p>Variation of the <math>BSe_{4/2}</math> (B=Ge,Si) corner-sharing mode frequency normalized to 1 in Raman spectroscopy with respect to the mean coordination number <math>\bar{r}</math>. The solid vertical lines define the intermediate phase in Ge-Se<sup>15</sup> while the lower solid line and the dashed line define it for Si-Se, following<sup>16</sup>. The Si Intermediate phase is larger than the Ge one. . . . .</p>	27
6	<p>The two local structures <math>Q^4</math> and <math>Q^3</math> in <math>(1-x)SiX_2 - xM_2X</math> glasses<sup>49</sup>, with <math>X = O, S, Se</math> and <math>M = Na, K, \dots</math>. The <math>Q^3</math> structure has one non-bridging anion. . . . .</p>	28
7	<p>Critical concentrations in <math>(1-x)SiX_2 - xM_2X</math> glasses, with <math>X = O, S, Se</math> and <math>M = Na, K, \dots</math>, as a function of the fraction of edge-sharing (ES) in the base <math>SiX_2</math> glass. The insert shows the corresponding width of the intermediate phase as a function of the same quantity. . . . .</p>	29

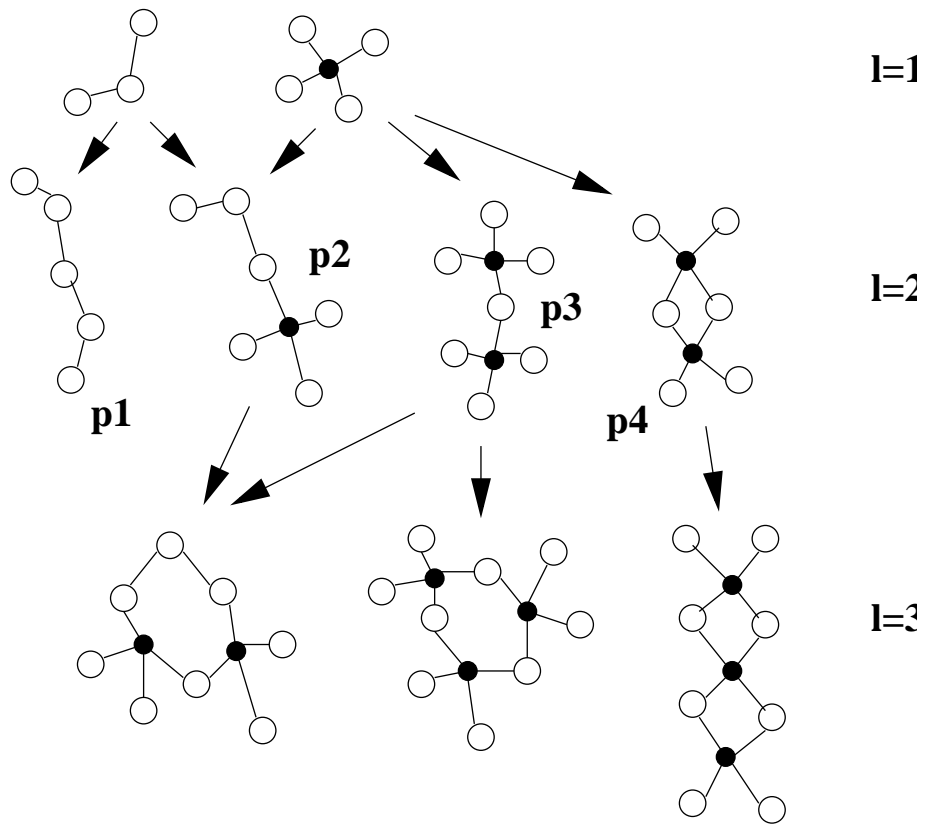


FIG. 1. From the short range order molecules ( $l = 1$ ) yielding the mean-field result to all clusters at  $l = 2$  and some MRO produced at  $l = 3$ . Isomers start to be created at step  $l = 3$ . Note the creation of medium range order such as edge-sharing tetrahedra or rings. Each boundary atom is counted half.

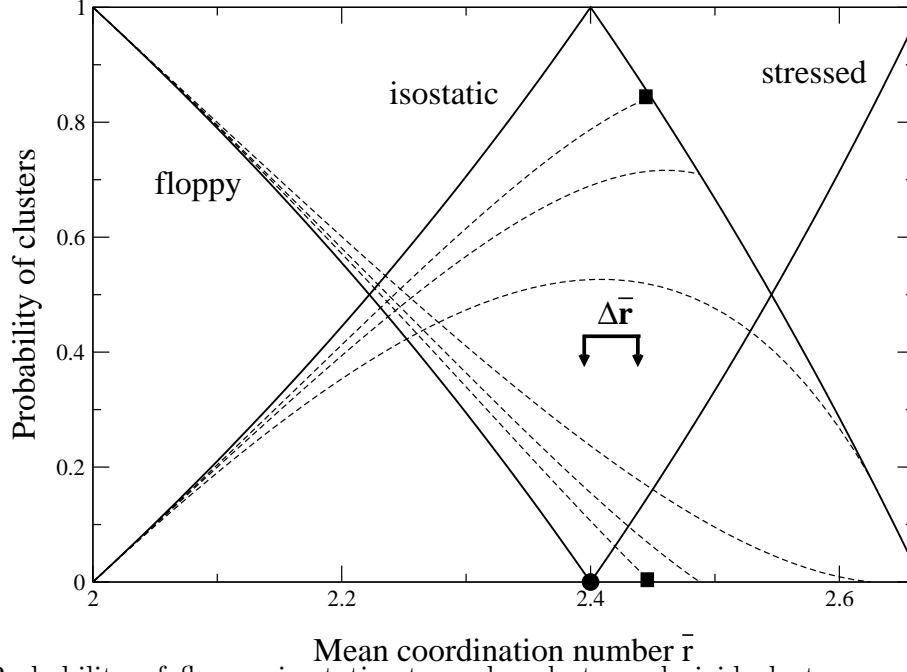


FIG. 2. Probability of floppy, isostatic stressed and stressed rigid clusters, as a function of the mean coordination number  $\bar{r}$  for different possibilities of medium range order. The solid line corresponds to the dendritic case while the broken lines correspond to a respective ES fraction at the stress transition of 0.156, 0.290 and 0.818. The filled square indicates the stress transition at the point  $\bar{r}_{c2}$  and the filled circle the point  $\bar{r}_{c1}$  that does not depend on the ES rate (see text for details). For clarity, we have removed the probabilities of stressed rigid clusters for non-zero ES fractions.



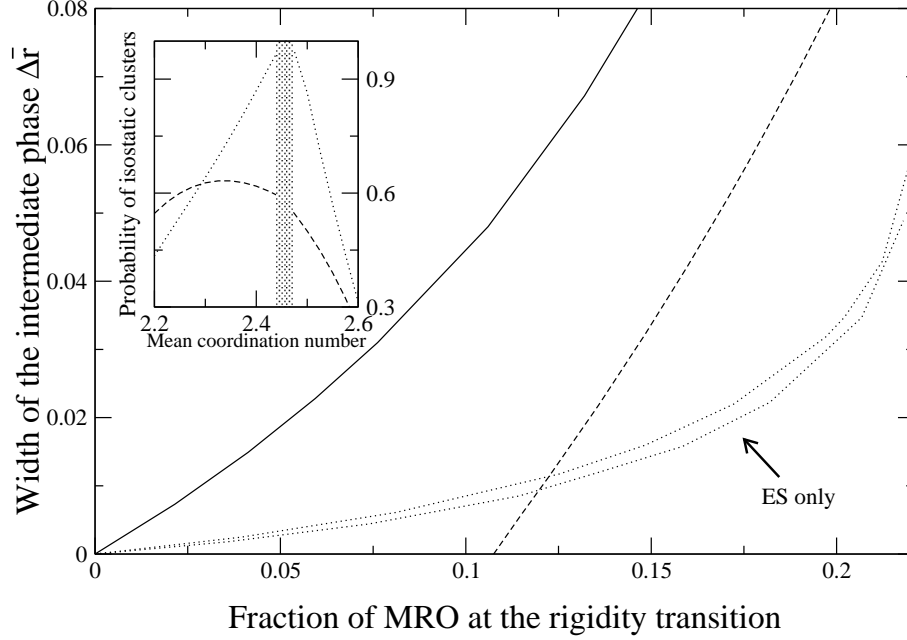


FIG. 3. Width of the intermediate phase as a function of the fraction of medium range order at the stress transition for  $l = 2$  (solid line),  $l = 3$  (dashed line) and  $l = 4$  (dotted lines). The lower dotted line corresponds to a structure where only ES tetrahedra have been allowed. The insert shows the probability of isostatic clusters with mean coordination number for  $l = 3$  (dashed line) and  $l = 4$  (dotted line), compared to the shaded region defined by the  $\Delta\bar{r}$  from SICA analysis. The point defined by  $f = 0$  is shifted compared to  $l = 2$ .

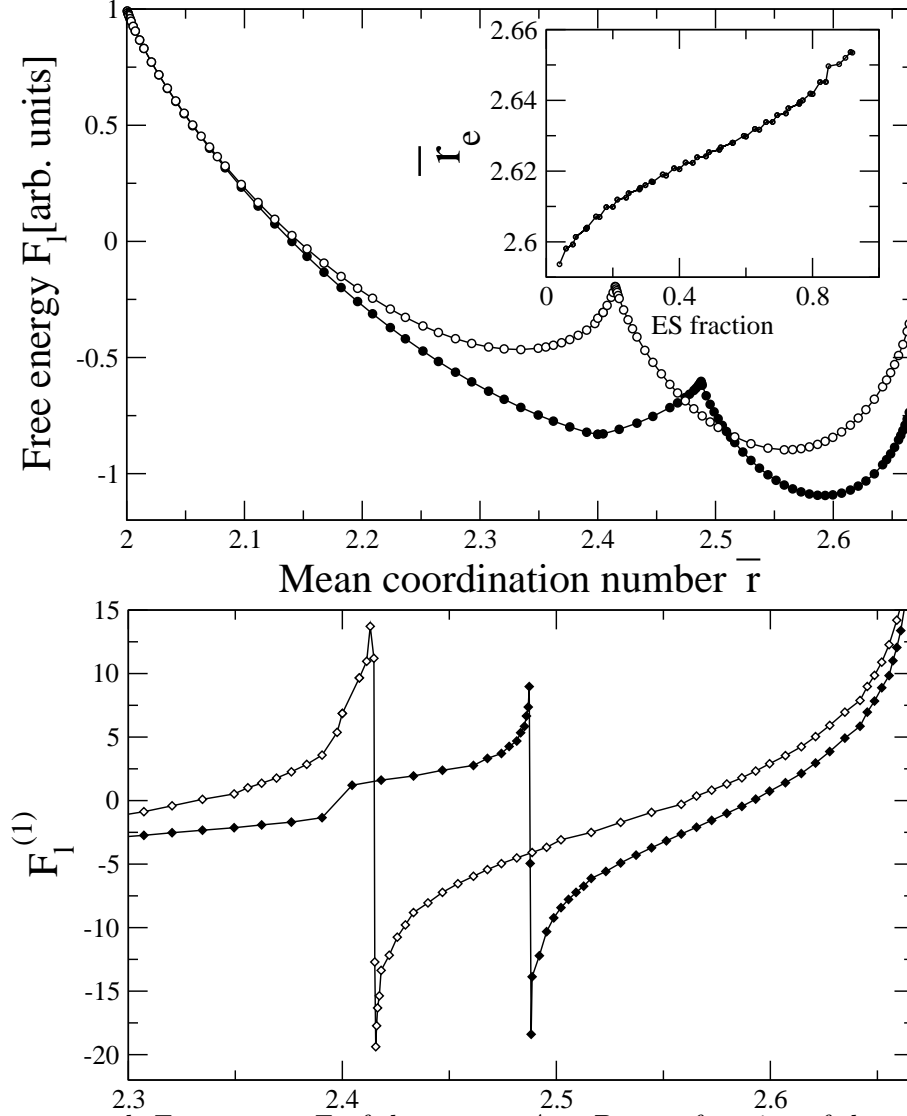


FIG. 4. Upper panel: Free energy  $F_l$  of the system  $A_{1-x}B_x$  as a function of the mean coordination number  $\bar{r}$  for different fractions of edge-sharing units  $\eta$ . Open circles:  $\eta = 0.29$ , filled circles:  $\eta = 0.56$ . The insert shows the equilibrium coordination number  $\bar{r}_e$  with respect to the ES fraction (see text for details). Lower panel: the first derivative of the free energy  $F_l^{(1)}$  with respect to  $\bar{r}$  as a function of  $\bar{r}$ .

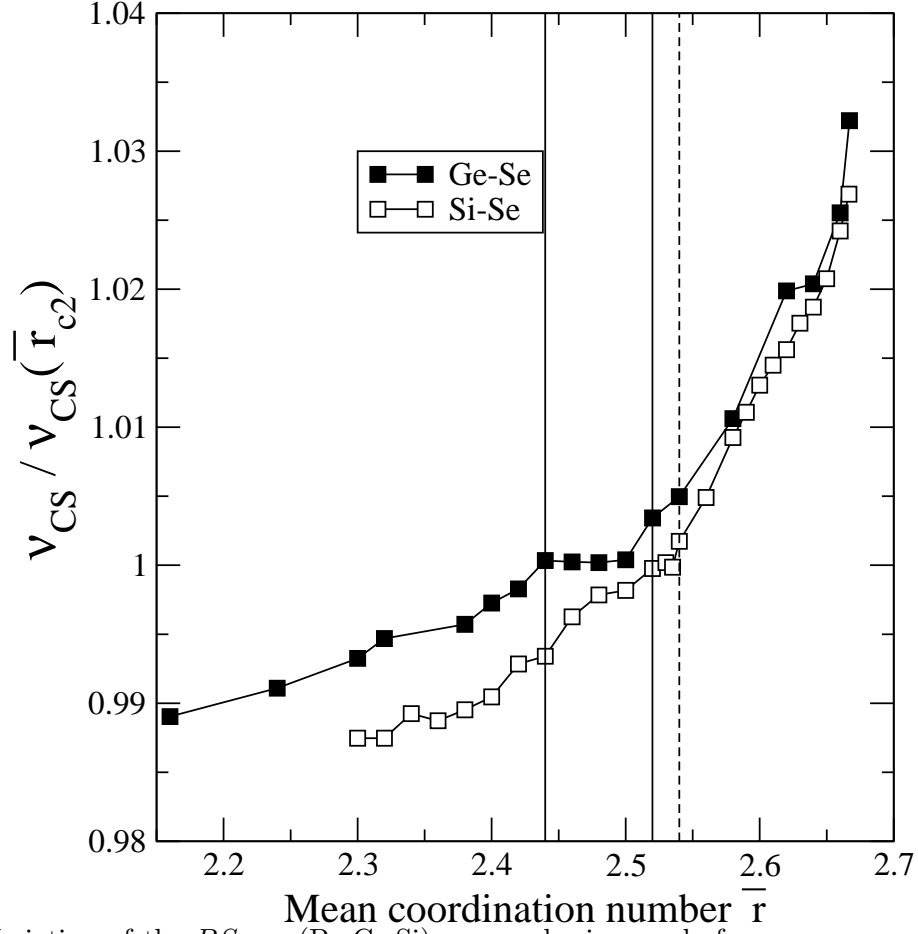


FIG. 5. Variation of the  $BSe_{4/2}$  (B=Ge,Si) corner-sharing mode frequency normalized to 1 in Raman spectroscopy with respect to the mean coordination number  $\bar{r}$ . The solid vertical lines define the intermediate phase in Ge-Se<sup>15</sup> while the lower solid line and the dashed line define it for Si-Se, following<sup>16</sup>. The Si Intermediate phase is larger than the Ge one.

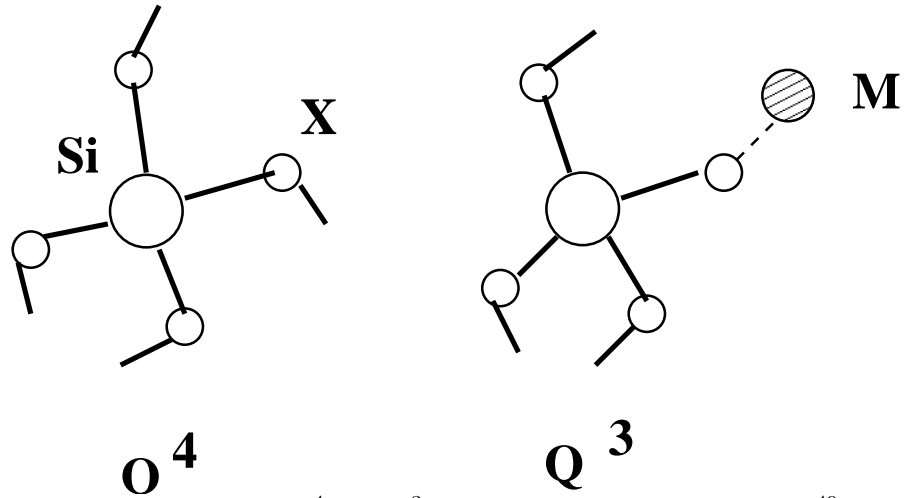


FIG. 6. The two local structures  $Q^4$  and  $Q^3$  in  $(1-x)SiX_2-xM_2X$  glasses<sup>49</sup>, with  $X = O, S, Se$  and  $M = Na, K, \dots$ . The  $Q^3$  structure has one non-bridging anion.

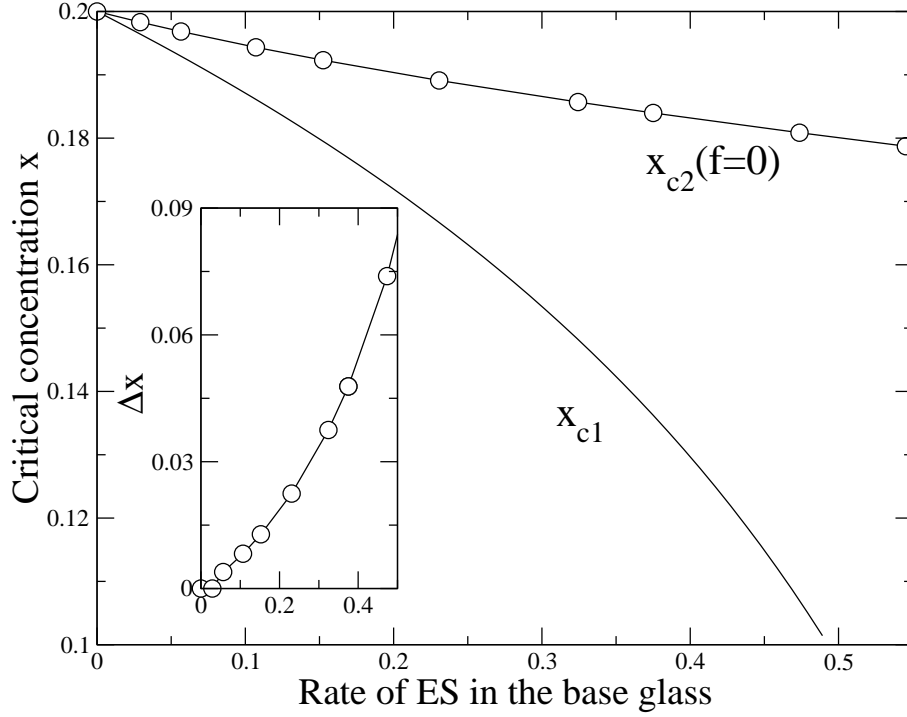


FIG. 7. Critical concentrations in  $(1 - x)SiX_2 - xM_2X$  glasses, with  $X = O, S, Se$  and  $M = Na, K, \dots$ , as a function of the fraction of edge-sharing (ES) in the base  $SiX_2$  glass. The insert shows the corresponding width of the intermediate phase as a function of the same quantity.